water

MDPI

Article

Application of Fe-Cu/Biochar System for Chlorobenzene Remediation of Groundwater in Inhomogeneous Aquifers

Xu Zhang, Yanqing Wu *, Pingping Zhao, Xin Shu, Qiong Zhou and Zichen Dong

School of Environmental Science and Engineering, Shanghai Jiao Tong University, 800 Dongchuan Road, Shanghai 200240, China; zick079@163.com (X.Z.); zhaopingping999@126.com (P.Z.); shuxin396064930@163.com (X.S.); 15821916726@126.com (Q.Z.); dongzichen@portqhd.com (Z.D.)

* Correspondence: wuyanqing@sjtu.edu.cn

Received: 25 October 2017; Accepted: 20 December 2017; Published: 25 December 2017

Abstract: Chlorobenzene (CB), as a typical Volatile Organic Contaminants (VOC), is toxic, highly persistent and easily migrates in water, posing a significant risk to human health and subsurface ecosystems. Therefore, exploring effective approaches to remediate groundwater contaminated by CB is essential. As an enhanced micro-electrolysis system for CB-contaminated groundwater remediation, this study attempted to couple the iron-copper bimetal with biochar. Two series of columns using sands with different grain diameters were used, consisting of iron, copper and biochar fillings as the permeable reactive barriers (PRBs), to simulate the remediation of CB-contaminated groundwater in homogeneous and heterogeneous aquifers. Regardless of the presence of homogeneous or heterogeneous porous media, the CB concentrations in the effluent from the PRB columns were significantly lower than the natural sandy columns, suggesting that the iron and copper powders coupled with biochar particles could have a significant removal effect compared to the natural sand porous media in the first columns. CB was transported relatively quickly in the heterogeneous porous media, likely due to the fact that the contaminant residence time is proportional to the infiltration velocities in the different types of porous media. The average effluent CB concentrations from the heterogeneous porous media were lower than those from homogeneous porous media. The heterogeneity retarded the vertical infiltration of CB, leading to its extended lateral distribution. During the treatment process, benzene and phenol were observed as the products of CB degradation. The ultimate CB removal efficiency was 61.4% and 68.1%, demonstrating that the simulated PRB system with the mixture of iron, copper and biochar was effective at removing CB from homogeneous and heterogeneous aquifers.

Keywords: chlorobenzene; Fe-Cu/biochar; PRBs; heterogeneous; removal

1. Introduction

Groundwater, as a water resource, is an important water supply helping to maintain ecosystem stability [1]. Groundwater contamination, due to the leakage and transport of organics, heavy metals and nitrates has triggered a widespread environmental problem [2,3]. Chlorinated solvents, are common organic contaminants, found at many contaminated sites, Chlorobenzene (CB) is one of the most ubiquitous chlorinated organic compounds found in contaminated groundwater; it is the main component in solvents, heat transfer agents, insect repellent, deodorant and is an intermediate in the pharmaceutical industry, also used during dye and pesticide synthesis [4,5]. Due to its toxicity, persistence, volatility and slow degradation [6,7], CB is an organic pollutant that is hard to remove from soil and groundwater [8]. Additionally, CB may threaten human health and damage organs via different exposure routes due to its widespread use [9]. For instance, people can be

exposed to CB-contaminated water through drinking, bathing, food and laundering. Public health concerns have arisen from the high volatility of CB, which results in various severe effects, including headaches, neurasthenia, dizziness, cyanosis, hyperesthesia, muscle spasms and increased risk of cancer [10]. Due to its high toxicity and ability to be accumulated in the human body and in the environment, CB has been listed as a controlled pollutant by the United States Environmental Protection Agency (USEPA) [11]. Therefore, CB-contaminated groundwater has become a worldwide health and environmental problem and developing an effective technology to treat the CB-contaminated groundwater is urgently required.

Permeable reactive barriers (PRBs), as passive in situ treatments, have been used as effective alternatives to remediate groundwater contaminated by organic and inorganic pollutants [12]. In a PRB, polluted groundwater transversely flows through a reactive material under natural hydraulic gradients wherein the contaminants are physically absorbed and chemically or biologically degraded [13,14]. An important step in constructing a PRB is choosing effective fillings. Various reactive materials have been used as fillings in PRBs for chlorinated component removal [15]. As one of the most common PRB fillings, zero-valent iron (ZVI) has been demonstrated to be an ideal and effective candidate for PRB to treat chlorinated compounds in groundwater [16]. However, the use of ZVI alone to remove organic contaminants has some shortcomings. Firstly, zero-valent iron particles are readily oxidized on surfaces in the ambient environment, resulting in the loss of active reaction sites [17]. Moreover, fine-sized iron powders are constantly unstable in aqueous solutions, causing their environmental application to be inconvenient [18]. Raw ZVI has low reactivity due to the passive layer generated during its manufacturing process, so the degradation rate for contaminant removal decreases over time, since its surface passivation is increased by the corrosion products such as iron hydroxide and oxides precipitant [19]. To enhance the reactivity of ZVI for the removal of organic contaminants, ZVI has been coupled with other materials, which has been proven effective for overcoming the ZVI shortcomings, improving its contaminant removal efficiency. Firstly, the addition of carbon materials reduces the possible contact between ZVI particles, consequently reducing the rapid formation of surface passivation and prolonging the effective life of Fe^0.

Biochar, as a solid heterogeneous material, is rich in aromatic carbon and minerals [20]. Due to its low production cost, high surface area, porosity and stable structure, biochar has been selected as a promising carbon material to facilitate the activity of ZVI [21,22]. ZVI coupled with biochar is defined as the iron/carbon (Fe^0/C) micro-electrolysis system. Fe^0/C micro-electrolysis primarily relies on the reaction of galvanic cells. ZVI, serving as the anode, releases electrons and the carbon materials, serving as active cathodes or facilitators, are commonly used in combination with iron chips to generate numerous local batteries in multiphase mixtures. Accordingly, reactions for decomposing refractory organics are believed to occur on or adjacent to the carbon surface [23]. Simultaneously, the addition of catalysts such as palladium (Pd), copper (Cu) and Nickel (Ni), onto the surface of Fe^0 to dechlorinate chlorinated hydrocarbons has aroused considerable research interest, due to having a better treatment effect than monometallic ZVI particles [24–26]. Among these catalysts, Pd exhibits the highest catalytic activity but its high cost may restrict its general application. Compared to Pd, Cu shows a distinct advantage over other noble metals because it is inexpensive [25,27]. In the bimetal systems, atomic hydrogen, a product of water splitting induced by iron corrosion, is proposed as the primary reductant for contaminants degradation. The Cu may serve as an effective reservoir for the atomic hydrogen to promote the degradation process [28]. Therefore, comparing to the single ZVI system, the Fe-Cu/biochar system is the preferred choice especially for in situ remediation when economics must be balanced with removal efficiency.

Additionally, many laboratory investigations into the in situ PRB remediation technologies have been conducted with homogeneous porous media [29,30]. However, the subsurface environment is a complex heterogeneous system. An aquifer is often composed of multi-layer geological materials with vastly different properties such as sand, silt and clay. The transport of organic pollutants is extremely complex due to the existence of heterogeneity in subsurface environment, making in situ

groundwater remediation in aquifers a challenging task. Many studies have reported on in situ remediation of organic contaminants in groundwater [31,32]. Due to the complexity and heterogeneity of an aquifer, application of these remediation technologies is limited. Prior flows are easily formed when contaminants flow by the highly permeable zones, whereas bypass flows are generated when contaminants flow through the low permeability zones. Herein, both phenomena may lead to the incomplete contact between contaminants and fillings in the PRB reaction zone [33–35]. In addition, after the reduction in the concentration of contaminants in highly permeable zones, under the force of concentration gradient, contaminants in low permeability zones are continuously released into highly permeable zones, increasing pollution and the cost of remediation [36,37]. Based on the above statement, comparing the treatment efficiency of PRB in homogenous and inhomogeneous porous media is essential, as it is significant for the application of PRB for in situ ground water remediation.

The objectives of this study were to apply the Fe-Cu/biochar system for in situ PRB remediation of CB in groundwater and to investigate the transport and removal process of CB in different subsurface porous media (homogeneous and heterogeneous media). The results could provide important reference data for the application of the Fe-Cu/biochar system for the in situ PRB remediation of groundwater in real applications.

2. Materials and Methods

2.1. Chemicals, Biochars and Sands

The biochars was prepared from pyrolysis of bamboos in the laboratory. The bamboo used in this work were collected from a park in Shanghai City, China. After washing for several times with tap water to remove adhered impurities, the bamboo was air-dried for 2 days and then oven-dried for 24 h at 120 °C. The dried bamboo was first chopped into small pieces and then milled by pestle, followed by sieving through 120 mesh. The average grain size of the biochar was 0.035–0.144 mm. Subsequently, pyrolysis was conducted in a muffle furnace (SX2-4-10) (Shanghai Shiyan electrical furnace Co., Ltd., Shanghai, China) which was supplied with nitrogen in order to maintain an oxygen-free atmosphere. During the pyrolysis process, the temperature was gradually increased at the rate of 45 °C per minute and finally maintained at 600 °C. Meanwhile, the nitrogen flow-rate was maintained at 200 mL/min. After reaching the target temperature, the sample was shifted into the operating furnace for 300 min. The resulting biochar was removed from the furnace, cooled, weighed and stored in airtight plastic containers until use.

The sands used in this study were coastal sediments obtained from the shoreline near Shanghai, China. Their texture and physio-chemical properties are similar to that of local confined aquifers. The sand was sieved into two different grain diameters: medium sand (M) and fine sand (F). The average grain size of the medium and fine sand was 0.153–0.459 and 0.055–0.125 mm, respectively.

Chlorobenzene (CB), iron and copper powders of analytical grade were purchased from Shanghai Sinopharm Chemical Reagent Co., Ltd., Shanghai, China. The average grain size of the iron and copper powders were 0.019–0.067 and 0.015–0.076 mm, respectively. Synthetic groundwater containing CB was prepared by adding CB into de-ionized water before use.

2.2. Column Test

The laboratory-scale column experiments designed for in situ PRB remediation were implemented and evaluated using two flow-through plexiglass columns 30 cm in height and an inner diameter of 4.1 cm. The columns were equipped with a constant head tank and a peristaltic pump to achieve steady flow conditions. Two nylon nets and porous sieve plates 1 cm in height were placed at the top and bottom to avoid sand erosion. Figure 1 illustrates the schematic diagram of the laboratory sequencing columns experiment system. In system A, the first column (column 1) was dry packed with fine sand simulating a homogeneous aquifer. The sand was first placed in the funnel and then allowed to fill the predetermined length of the tubing. The columns were gently tapped until the desired amount

of sands was placed in the column. The second column (column 2) was packed with fine sand as the matrix and the middle of the column was filled to a height of 9.8 cm with the reactive barrier containing the mixture of 56.8 g iron powder, 5.7 g copper powder and 28.4 g biochar. The depth of the sand layer above and beneath the reactive layer was 9.1 cm. The Fe-Cu/biochar mixture was prepared by mixing the iron, copper and biochar powders together to form a homogeneous mixture using stirrer. In system B, fine and medium sands were sequentially dry packed into the column 1 and each occupied 50% of the available volume. The second column was sequentially packed with medium and fine sands as the matrix and the middle of the column was filled with a reactive barrier containing the mixture of iron, copper, biochars powders with the same mass and composition as in system A. The first columns of both systems could be also regarded as control tests to observe the adsorption and interception effects by the natural sand porous media. The specifications of the experimental setup and basic parameters are listed in Tables 1 and 2.

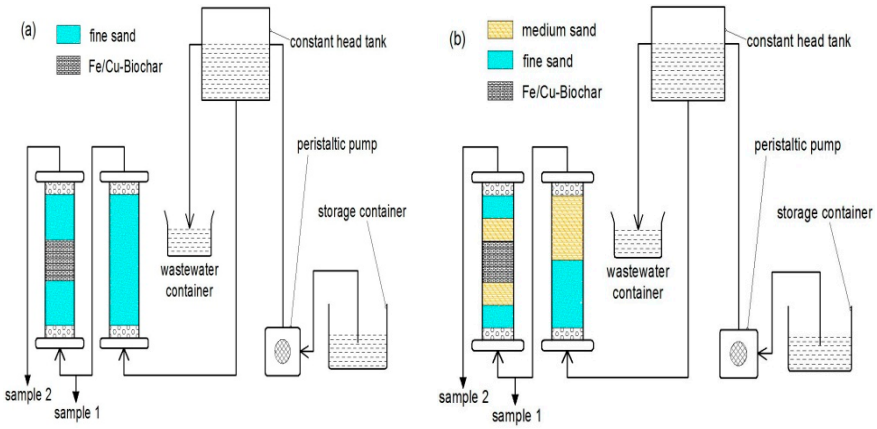

Figure 1. Schematic diagram of the experimental apparatus: (**a**) contaminant transport and removal experiment in a saturated homogeneous columns system; and (**b**) contaminant transport and removal experiment in saturated heterogeneous columns.

Table 1. Experimental configurations and specifications of the applied homogeneous systems.

Media Type	Column Code	Components	Porosity	Particle Diameter (mm)
Homogeneous	1	F	0.411	0.055–0.125
Homogeneous	2	Fe	0.317	0.019–0.067
Homogeneous	2	Cu	0.317	0.015–0.076
Homogeneous	2	B	0.317	0.035–0.144
Homogeneous	2	F	0.317	0.055–0.125

Note: F represents fine sand, F + M presents fine sand with medium sand, Fe presents iron powders, Cu presents copper powders and B presents biochar particles.

Table 2. Experimental configurations and specifications of the applied heterogeneous systems.

Media Type	Column Code	Components	Porosity	Particle Diameter (mm)
Heterogeneous	1	M + F	0.429	0.046–0.454
Heterogeneous	2	Fe	0.339	0.019–0.067
Heterogeneous	2	Cu	0.339	0.015–0.076
Heterogeneous	2	B	0.339	0.035–0.144
Heterogeneous	2	M + F	0.339	0.046–0.454

Note: F represents fine sand, F + M presents fine sand with medium sand, Fe presents iron powders, Cu presents copper powders and B presents biochar particles.

Before the experiment, columns were first flushed with numerous volumes of deionized water to saturate the sand columns to remove the air in the columns, followed by introducing NaCl solution as

conservative tracer into columns to analyze the hydrodynamic behavior of the PRB system columns. The conductivity meter (Myron L Company, Carlsbad, CA, USA) was used to determine the effluent solute conductivity. The CB synthetic groundwater was continuously introduced into the column using the peristaltic pump. Meanwhile, the constant head tank was used to maintain the transport system in a constant hydraulic head condition. The variations in effluent CB concentrations from columns 1 and 2, pH and total iron ions concentrations from column 2 were collected at predetermined time intervals. All experiments were repeated three times and the average values are presented.

The water solution containing 38.85 mg/L of CB was prepared to simulate CB-contaminated groundwater. Samples were taken from the outlets at predetermined time intervals.

2.3. Characterization

Scanning electron microscope (SEM) (Sirion 200) (FEI Company, Hillsboro, OR, USA) images were used to analyze the micro-structure of the samples that were captured using a scanning microscope to compare the interior and surface characteristics of the samples.

The mineral compositions of the samples were also characterized using X-ray Diffraction (XRD) analysis to identify crystalline structures in the Fe-Cu/biochar system using a computer-controlled X-ray diffractometer (XRD) (XRD-6100) (Shimadzu, Kyoto, Japan) equipped with a stepping motor and graphite crystal monochromator.

2.4. Analytical Methods

CB effluent concentrations were quantified by using 20 mL headspace samples that were analyzed by a gas chromatograph (GC-2010) (Shimadzu, Kyoto, Japan) using a flame photometric detector that was used for separation and determination of organic contaminants. The intermediates of the CB were qualitatively analyzed using the gas chromatography-mass spectrometer (GC-MS-QP 2010) (Shimadzu, Kyoto, Japan). The concentrations of iron ions from the second columns of both systems were determined by use of an Inductively Coupled Plasma Optical Emission Spectrometer (ICP-PS3500DD) (Hitachi, Kyoto, Japan). The pH values of the second columns were measured using a pH meter (PHS-3C) (Shanghai Yidian Scientific Instrument Co., Ltd., Shanghai, China).

3. Discussion

3.1. Characterization of the Fe-Cu/Biochar System

To obtain the surface morphology of the system, the SEM characterization of Fe-Cu/biochar was completed. In Figure 2, the SEM image of Fe-Cu/biochar revealed that the bamboo was completely carbonized and tiny carbon sticks or slices were presented. The surface of the Fe-Cu/biochar system were rough and some apertures existed with different pore sizes and diverse pore distributions, causing their rough surface and increasing their specific surface area. Small particles were unevenly distributed on the surface of the biochar and inside the pores, demonstrating the existence of iron and copper powders on the surface of the biochar. This means that the iron and copper powders were effectively mixed with the biochar.

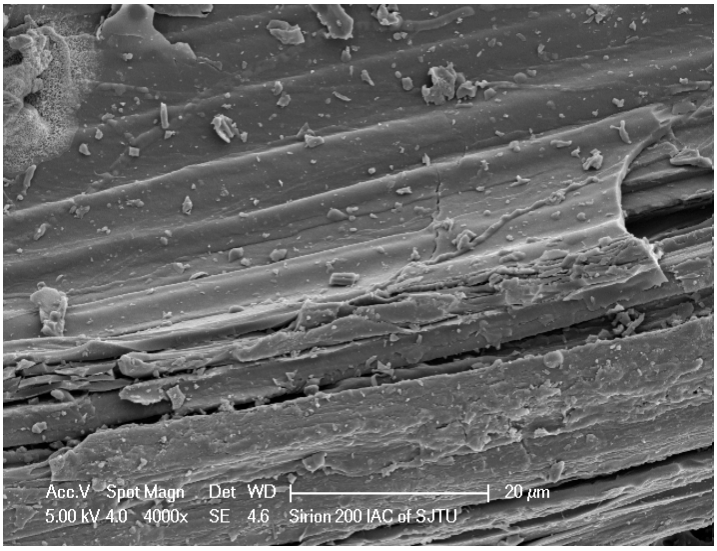

Figure 2. Scanning electron microscope (SEM) images of the morphological structure of the Fe-Cu/biochar system.

The structure and phase composition of the Fe-Cu/biochar system before and after treatment were investigated using XRD analysis. As shown in Figure 3, the wide diffraction peak at a small angle might be attributed to the amorphous phase of the biochar that was apparent in the samples. The apparent peaks at 43.36° and 64.99° are the characteristic diffraction peaks of iron, which confirmed the presence of iron in its zero-valent state. Only one peak at 74.15°, representing the crystal structure of copper, was clearly confirmed for the presence of high purity. After the Fe-Cu/biochar system treatment, two new characteristic diffraction peaks appeared at 44.70° and 50.44°, implying the generation of iron oxides during the reaction process.

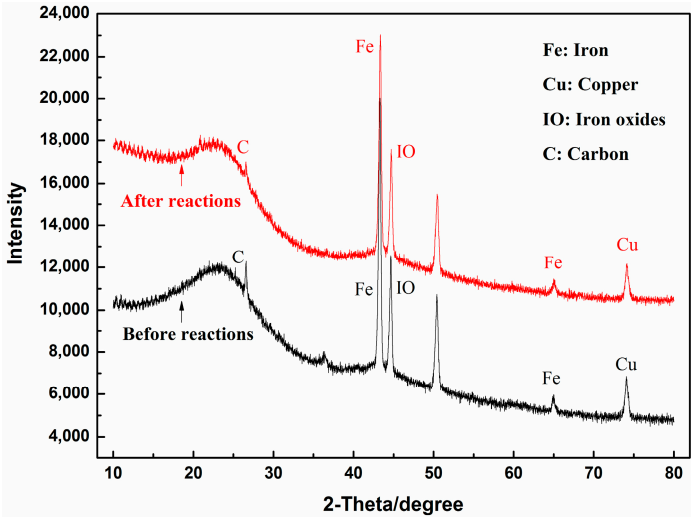

Figure 3. X-ray Diffraction (XRD) images of the Fe-Cu/biochar system.

Figure 4 shows the XRD diffraction patterns for medium and fine sands. Results from the XRD analysis identified the medium and fine sands in the XRD patterns. The main diffraction peaks of the medium and fine sands were observed at 20.98°, 26.72°, 40.47°, 50.26° and 68.15° and 22.67°, 26.91°, 50.36°, 60.19° and 68.34°, respectively, meaning the main mineral in the medium and fine sands was silicon dioxide.

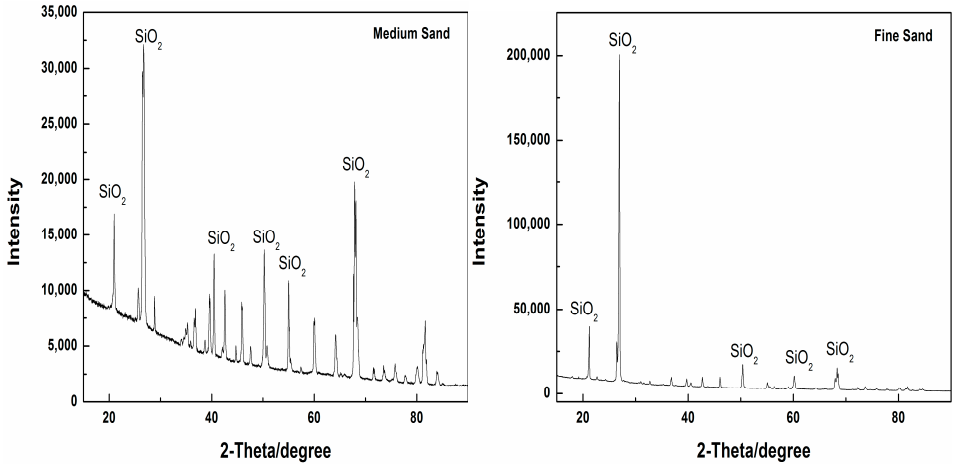

Figure 4. XRD images of the medium and fine sands.

3.2. Column Tests in Homogeneous and Heterogeneous Porous Media

Figures 5 and 6 display the CB concentrations in the effluent versus treatment times from the columns of the two systems, representing the ratio between the CB concentration in the column outlet with its concentration at the column inlet. The trend of the variation in effluent CB concentrations were similar for the first column of both systems. The effluent CB concentrations in heterogeneous porous media (system B) was detected at about 1.2 Pore Volumes,(PV), which was comparable to that found in the homogeneous porous media (system A) at about 1.9 PV. It is probably because the homogeneous system A had lower porosity and less dispersion, so more organic contaminants were held in the media due to capillary condensation in column 1 of the homogeneous system A. The changes in CB concentrations sharply increased from about 2.9 to 4.6 PV and 2.7 to 4.8 PV in the first columns of systems A and B, respectively. After the rate of increase of the effluent CB concentrations became steady. The changes in effluent CB concentrations did not exhibit a continuous downtrend during the period, meaning that insignificant CB removal occurred in the first column effluents of both systems. Consequently, the CB removal was extremely low in the natural sand media. The sand did not react with CB, meaning the sand and the CB solution might have complex adsorption and desorption process.

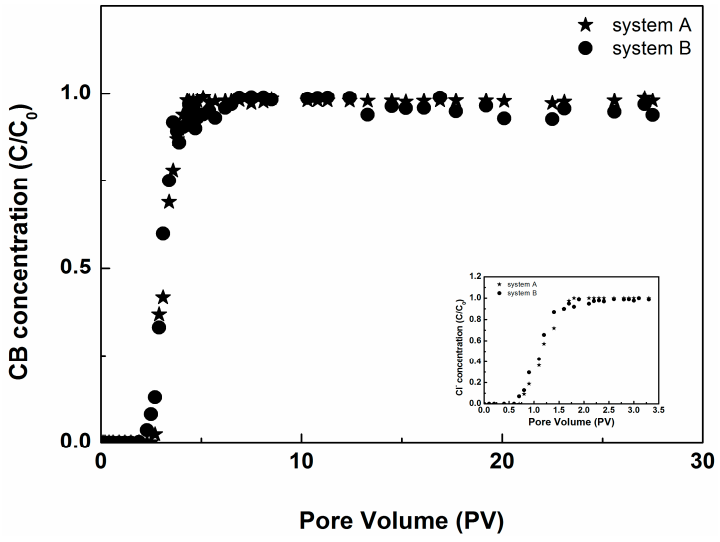

Figure 5. Variations in CB concentration profiles over times for column one of both systems. The inset displays the breakthrough curve of a sodium chloride (NaCl) tracer.

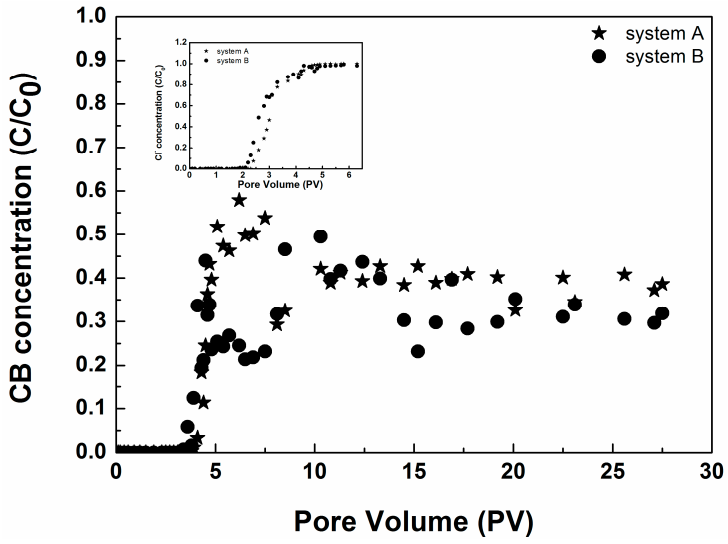

Figure 6. Variations in CB concentration profiles over times for column two of both systems. The inset displays the breakthrough curve of a sodium chloride (NaCl) tracer.

For the second columns of both systems, the mixture of iron and copper powders and biochar particles reacted with CB when CB solution flowed through this permeable reactive barrier. Although the influent CB concentration was 38.85 mg/L, the effluent CB concentrations were lower in both second columns of systems A and B. The effluent CB concentrations in both second columns were significantly low compared to the first columns, indicating that the iron and copper powders coupled with biochar particles have a palpable removal effect compared to the natural sand porous media in the first columns. Additionally, compared to the PRB fillings of the second columns, the natural aquifer materials were unlikely to have a significant impact on effluent concentrations because the hydraulic conductivity of the PRB is greater than that of the aquifer. Here, the PRB provides a preferential connection between the permeable units of the influent and effluent faces [38]. Nevertheless, the concentration changes in the effluents of the second columns between homogeneous system A and heterogeneous systems B were different. Initially, the CB effluent concentrations in systems A and B were extremely low and an insignificant increase and decrease was observed in the effluents of both systems, associated with the initial solid adsorption equilibrium process occurring in the aquifer materials and PRB fillings. After this period, the effluent concentrations in systems A and B increased from about 4.1 and 3.8 PV, reaching a maximum value of about 6.2 and 10.3 PV, respectively. Subsequently, the effluent CB concentration in heterogeneous system B was more unstable and variable compared to system A, until the end of treatment.

Notably, the effluent CB concentrations in both systems were relatively stable and not very high at the end of the experiment. The average residence time in the heterogeneous porous media was shorter compared to the homogeneous porous media. The contaminant's residence time is associated with the infiltration velocities of the homogeneous or heterogeneous porous media rather than the innate hydraulic conductivity of the PRB in homogeneous system A or the heterogeneous porous media in system B [38]. Additionally, in the heterogeneous porous media, a slight curvature of the path lines was generated near the edges of the reactive barrier, indicating a modestly higher gradient in this region. Therefore, the residence times of the contaminants were slightly shorter in the permeable reactive barrier reaction zone. Once contaminants exited the barrier and entered the aquifer, they dispersed into a plume that was wider than the reactive barrier. The average effluent CB concentration of the heterogeneous porous media was lower than that of the homogeneous porous media. We speculate that the heterogeneity retarded the vertical infiltration of CB, leading to its extended lateral spread. Compared to the homogeneous porous media, the layered heterogeneous porous media combined

with the Fe-Cu/biochar system increased the lateral spread of the CB distribution, thereby lowering the effluent CB concentration [39].

Figures 5 and 6 show the breakthrough curves of the tracer experiments, representing the ratio between the concentration of sodium chloride (NaCl) in the column outlet to its concentration in the column inlet, denoted by ratio between current and initial concentration (C/C_0). As shown in Figures 5 and 6, the mass transfer process of chloride (Cl^-) tracer in heterogeneous system B was much faster than in homogeneous system A. Also, the transport of NaCl tracer was much faster than CB in both systems, indicating the sands and the PRB did not have an obvious retardation effect on the conservative tracer.

At the end of the experiment, the CB removal efficiency was at 61.4% and 68.1%, considered effective for both the homogeneous and heterogeneous columns effluents, respectively. The destruction of CB by the Fe-Cu/biochar system was a heterogeneous reaction, involving the micro-electrolysis, catalysis and adsorption process throughout the entire treatment. In the Fe-Cu/biochar system, the iron powders served as an anodic metal that provided electrons for CB destruction. Biochar particles worked as cathodes to generate macroscopic galvanic cells when in contact with iron particles, significantly accelerating the corrosion of iron and stimulating the release of more iron ions and electrons [23]. The addition of copper increases the potential difference between the anode and cathode, which in principle boosted the treatment efficiency [40]. Additionally, copper covering on the iron surface accelerated the corrosion of ZVI and the generation of hydrogen ions ([H]) [41]. As the entire reaction occurred in an alkaline environment, iron corrosion products such as $Fe(OH)_2$, $Fe(OH)_3$, FeOOH, Fe_2O_3 and Fe_3O_4 or green rusts might be generated during the iron corrosion process and the contaminants could be eliminated to some extent through these corrosion products with adsorptive and agglomerate characteristics [42]. Moreover, the generation of these corrosion products might be enhanced by Cu catalysis and the adsorption and co-precipitation effect would be accordingly improved. However, in the alkaline environment, the iron corrosion process was inhibited and the generation of iron corrosion products decreased, resulting in a weak reduction, coagulation and adsorption effect [41].

3.3. Released Iron Ion Concentration in Effluents

Iron ions are an important form of iron in aqueous environments. Hence, monitoring the variations in the iron ion concentrations in the effluents of the second columns of systems A and B was important during the treatment. The results shown in Figures 7 and 8 demonstrate that the iron ion concentrations in the effluent of both systems was initially almost undetectable, gradually increasing to maximum values of 8.722 and 9.479 mg/L at about 13.3 and 7.5 PV for systems A and B, respectively, because iron ions formed during the electrolysis process and were released from the PRB reaction zone into the solution. The maximum iron concentration in system B occurred later than in the homogeneous system but the maximum was higher than that of system A. With the longer treatment time, the effluent Fe concentration decreased drastically with very low levels observed by the end of the entire treatment, the consumed iron ions might be used for the activation of degradation process. At the last period, iron ions reacted with OH^- to form precipitations, inducing the decrease of iron ions concentrations in the solution. By the end of the treatment, the iron ions concentrations were 0.093 and 0.059 mg/L for systems A and B, respectively, which meet the quality standard for groundwater (GB/T 14848-93, China) [43].

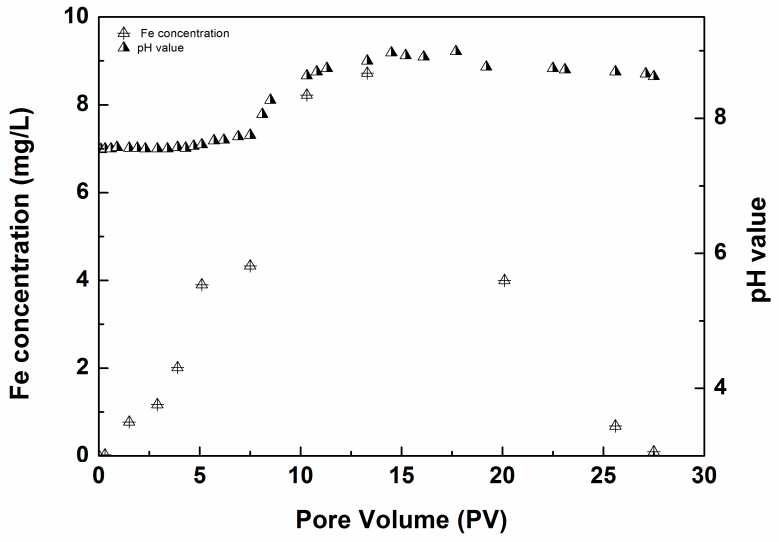

Figure 7. Variations in iron ion concentrations and pH profiles over time in the second columns of the homogeneous porous media in system A.

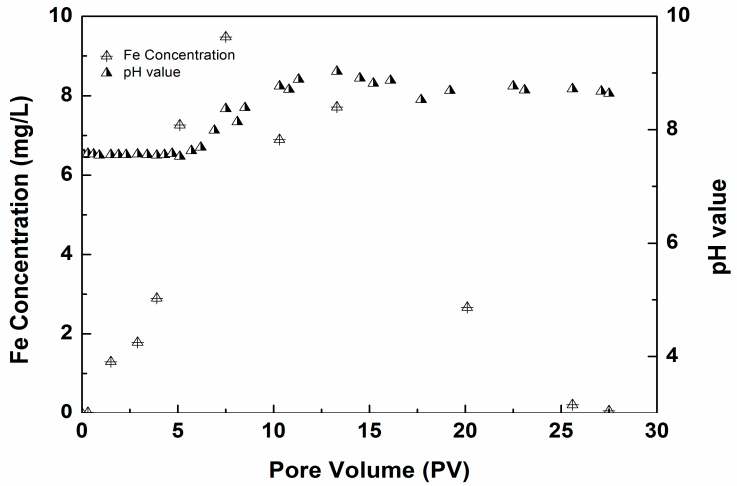

Figure 8. Variations in iron ion concentrations and pH profiles over time in the second columns of the heterogeneous porous media in system B.

3.4. pH Changes of the Effluents

Figures 7 and 8 shows the effluent pH versus time in the effluents of the Fe-Cu/biochar treatment column of systems A and B, respectively. The influent pH was 7.55, which was approximately equal to the actual value in groundwater. The effluent pH in system A, where homogeneous sand was used as the matrix, increased to almost 9, remained steady until about 17.7 PV. Then pH dropped slowly, reaching 8.62 by the end of the test. The effluent pH in system B, where medium and fine sand was used as the matrix, increased to about 9 and remained at this value until about 13.3 PV. Subsequently, the pH initially showed a down-up trend and subsequently stabilized by the end of the test. At the initial stage, the pH values of both systems were relatively stable, likely because the CB solutions underwent an initial solid adsorption equilibrium process when flowing through systems A and B. After the pH value reached a maximum in system B, occurring later than in system A, reflecting the flow heterogeneity development over treatment time. In the middle of the treatment in both systems, the H^+ ions in the solution were obvious consumed due to the catalytic micro-electrolysis activity, causing the relatively fast increase in pH values. At the end, the decrease in pH might be attributed to

the reaction between the iron ions and OH^- to form a precipitation, which consequently resulted in the decrease of the pH value in the system.

3.5. Intermediates of CB-Contaminated Groundwater

After approximately 12 PV of treatment, the effluent from the second column of the heterogeneous system was collected and qualitatively analyzed using GC/MS. As shown in Figure 9, benzene and phenol were found to be the major intermediate products of the heterogeneous system. For the Fe-Cu/biochar system treatment of CB-contaminated groundwater, several mechanisms were responsible for its degradation. Among them, the two significant degradation paths displayed in Figure 10 were mainly responsible for the CB degradation in the Fe-Cu/biochar system. The first path was the reduction effect by the reductants (hydrogen radical ([H]), Fe^0 and Fe^{2+}) generated from the iron corrosion process [44], contributing to the main product of benzene in the Fe-Cu/biochar system. This path, has also been proven in prior studies [45,46]. The second path was the oxidation effect by strong oxidants (hydroxyl radical [OH]) generated from Fenton reactions in the Fe-Cu/biochar system when oxygen is introduced into the system, giving rise to the formation of phenol [47,48]. Both the above reduction and oxidation effect would both reduce the toxicity of CB [48]. Secondly, the adsorption and co-precipitation from iron (hydro) oxides had a minor effect on the removal of the organic contaminants, which might be generated with longer reaction times or higher pH. Moreover, absorption from the biochar could remove some organic contaminants in the solution; however, this effect would considerably weaken as the saturation adsorption was attained with longer reaction time.

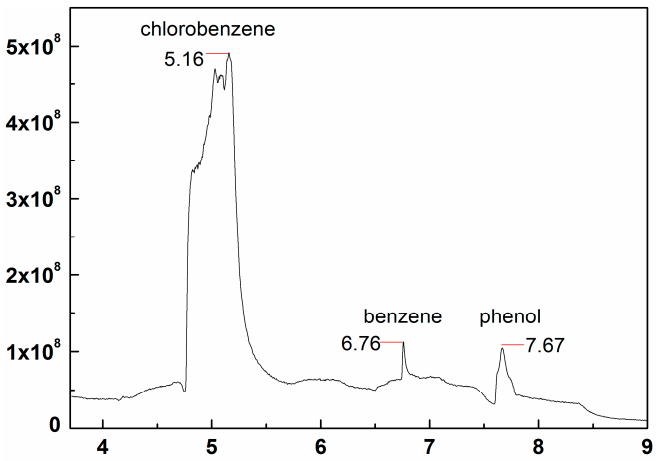

Figure 9. The Chlorobenzene intermediates during the Fe-Cu/biochar treatment.

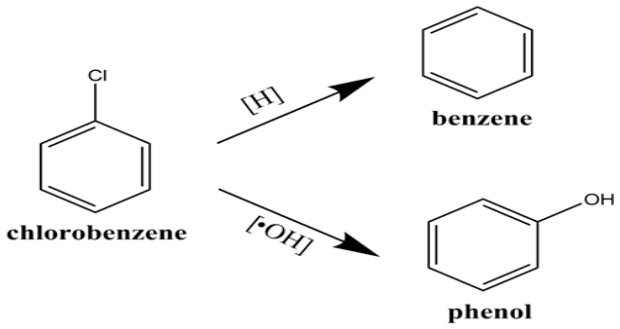

Figure 10. The main chlorobenzene degradation mechanisms during the Fe-Cu/biochar treatment.

4. Conclusions

In this study, the Fe-Cu bimetal system coupled with a biochar material barrier was investigated and applied to remediate CB-contaminated groundwater.

Regardless of the homogeneity or heterogeneity of the porous media, the effluent CB concentrations from the PRB columns were significantly low compared to the natural sandy columns, illustrating that the iron and copper powders coupled with biochar particles had a palpable removal effect compared to the natural sand porous media in the first columns. The PRB itself provided a preferential connection between permeable units of the influent and effluent faces. On average, the CB was transported relatively quickly in the heterogeneous porous media, which might be due to fact that the residence time of contaminants was proportional to the infiltration velocities in the different types of porous media and not the hydraulic conductivity of the PRB. For the heterogeneous porous media, a slight curvature of the path lines appeared near the edges of the reactive barrier and a slightly higher gradient occurred in this region, consequently leading to a shorter CB resident time in the PRB reaction zone.

The average effluent CB concentrations of the heterogeneous porous media were lower than in the homogeneous porous media, which was possibly due to the heterogeneity limiting the vertical infiltration of CB, leading to its extended lateral spread. The ultimate CB removal efficiency was 61.4% and 68.1% in the homogeneous and heterogeneous columns effluents, respectively, exhibiting a satisfactory CB removal efficiency. This result should be ascribed to the treatment with the Fe-Cu/biochar system that involved micro-electrolysis, catalysis and adsorption. The addition of copper powder increases the iron corrosion, effectively remediating the CB-contaminated groundwater. By the end of the treatment, the iron ion concentrations were 0.093 and 0.059 mg/L in systems A and B, respectively, which are within the quality standard for groundwater (GB/T 14848-93, China). The pH variations were relatively stable at the initial stage, when the CB solutions encountered the initial solid adsorption equilibrium process. The pH value reached its maximum in system B at a later time than that of system A, implying flow heterogeneity development over treatment time. Benzene and phenol were observed as the products of CB degradation in the column tests. During the Fe-Cu/biochar treatment process, two degradation paths might play a role in the removal of CB. One path is the reduction effect, responsible for the production of benzene. The other is the oxidation effect, which induced the formation of phenol.

Acknowledgments: This research was supported by the National Natural Science Foundation of China (41272261) and Shanghai Science and Technology Project (15DZ1205803). The authors are grateful to the reviewers who helped us improve the paper by many pertinent comments and suggestions.

Author Contributions: Xu Zhang and Yanqing Wu conceived and designed the experiments; Xu Zhang and Pingping Zhao performed the experiments; Xin Shu analyzed the data; Xu Zhang wrote the paper; Zichen Dong and Qiong Zhou conducted the English correction.

Conflicts of Interest: The authors declare no conflict of interest.

References

1. Morris, B.L.; Lawrence, A.; Chilton, J.; Adams, B.; Calow, R.C.; Klinck, B.A. *Groundwater and Its Susceptibility to Degradation: A Global Assessment of the Problem and Options for Management*; British Geological Survey: Nottingham, UK, 2003.
2. Liu, Y.; Mou, H.; Chen, L.; Mirza, Z.A.; Liu, L. Cr(VI)-contaminated groundwater remediation with simulated permeable reactive barrier (PRB) filled with natural pyrite as reactive material: Environmental factors and effectiveness. *J. Hazard. Mater.* **2015**, *298*, 83–90. [CrossRef] [PubMed]
3. Stroo, H.F.; Leeson, A.; Marqusee, J.A.; Johnson, P.C.; Ward, C.H.; Kavanaugh, M.C.; Sale, T.C.; Newell, C.J.; Pennell, K.D.; Lebrón, C.A. Chlorinated ethene source remediation: Lessons learned. *Environ. Sci. Technol.* **2012**, *46*, 6438–6447. [CrossRef] [PubMed]

4. Blad, M.C.; Gutierrezwing, M.T.; Constant, W.D. Characterization of mass transfer of lower chlorinated benzenes from contaminated sediment into water. *J. Hazard. Mater.* **2012**, *221–222*, 109–117. [CrossRef] [PubMed]
5. Oh, Y.S.; Bartha, R. Design and performance of a trickling air biofilter for chlorobenzene and o-dichlorobenzene vapors. *Appl. Environ. Microbiol.* **1994**, *60*, 2717–2722. [PubMed]
6. Braune, B.M.; Outridge, P.M.; Fisk, A.T.; Muir, D.C.G.; Helm, P.A.; Hobbs, K.; Hoekstra, P.F.; Kuzyk, Z.A.; Kwan, M.; Letcher, R.J. Persistent organic pollutants and mercury in marine biota of the Canadian Arctic: An overview of spatial and temporal trends. *Sci. Total Environ.* **2005**, *351–352*, 4–56. [CrossRef] [PubMed]
7. Maria, G.; Maria, C. A review of accidental release simulated case studies on dispersion and bioaccumulation of PCB and CB persistent pollutants in riverbeds. *Rev. Chim. Bucharest Orig. Ed.* **2009**, *60*, 699–705.
8. Oliver, B.G.; Nicol, K.D. Chlorobenzenes in sediments, water and selected fish from Lakes Superior, Huron, Erie and Ontario. *Environ. Sci. Technol.* **1982**, *16*, 260–286. [CrossRef]
9. Harper, D.J.; Ridgeway, I.M.; Leatherland, T.M. Concentrations of hexachlorobenzene, trichlorobenzenes and chloroform in the waters of the Forth Estuary, Scotland. *Mar. Pollut. Bull.* **1992**, *24*, 244–249. [CrossRef]
10. Ogata, M.; Taguchi, T.; Hirota, N.; Shimada, Y.; Nakae, S. Quantitation of urinary chlorobenzene metabolites by HPLC: Concentrations of 4-chlorocatechol and chlorophenols in urine and of chlorobenzene in biological specimens of subjects exposed to chlorobenzene. *Int. Arch. Occup. Environ. Health* **1991**, *63*, 121–128. [CrossRef] [PubMed]
11. Wang, J. Chlorobenzene degradation by electro-heterogeneous catalysis in aqueous solution: Intermediates and reaction mechanism. *J. Environ. Sci.* **2008**, *20*, 1306–1311. [CrossRef]
12. Tosco, T.; Papini, M.P.; Viggi, C.C.; Sethi, R. Nanoscale zerovalent iron particles for groundwater remediation: A review. *J. Clean. Prod.* **2014**, *77*, 10–21. [CrossRef]
13. Do, S.H.; Kwon, Y.J.; Kong, S.H. Feasibility study on an oxidant-injected permeable reactive barrier to treat BTEX contamination: Adsorptive and catalytic characteristics of waste-reclaimed adsorbent. *J. Hazard. Mater.* **2011**, *191*, 19–25. [CrossRef] [PubMed]
14. Rivett, M.O.; Chapman, S.W.; Allen-King, R.M.; Feenstra, S.; Cherry, J.A. Pump-and-Treat Remediation of Chlorinated Solvent Contamination at a Controlled Field-Experiment Site. *Environ. Sci. Technol.* **2006**, *40*, 6770–6781. [CrossRef] [PubMed]
15. Liang, S.H.; Chen, K.F.; Wu, C.S.; Lin, Y.H.; Kao, C.M. Development of $KMnO_4$-releasing composites for in situ chemical oxidation of TCE-contaminated groundwater. *Water Res.* **2014**, *54*, 149–158. [CrossRef] [PubMed]
16. Kebria, D.Y.; Taghizadeh, M.; Camacho, J.V.; Latifi, N. Remediation of PCE contaminated clay soil by coupling electrokinetics with zero-valent iron permeable reactive barrier. *Environ. Earth Sci.* **2016**, *75*, 1–11. [CrossRef]
17. Feitz, A.J.; Joo, S.H.; Guan, J.; Sun, Q.; Sedlak, D.L.; Waite, T.D. Oxidative transformation of contaminants using colloidal zero-valent iron. *Colloids Surf. Physicochem. Eng. Asp.* **2005**, *265*, 88–94. [CrossRef]
18. Zhang, W.X. Nanoscale Iron Particles for Environmental Remediation: An Overview. *J. Nanopart. Res.* **2003**, *5*, 323–332. [CrossRef]
19. Joo, S.H.; Feitz, A.J.; Sedlak, D.L.; Waite, T.D. Quantification of the oxidizing capacity of nanoparticulate zero-valent iron. *Environ. Sci. Technol.* **2005**, *39*, 1263–1268. [CrossRef] [PubMed]
20. Lehmann, J. A handful of carbon. *Nature* **2007**, *447*, 143–144. [CrossRef] [PubMed]
21. Yao, Y.; Gao, B.; Chen, J.; Zhang, M.; Inyang, M.; Li, Y.; Alva, A.; Yang, L. Engineered carbon (biochar) prepared by direct pyrolysis of Mg-accumulated tomato tissues: Characterization and phosphate removal potential. *Bioresour. Technol.* **2013**, *138*, 8–13. [CrossRef] [PubMed]
22. Zhang, M.; Gao, B. Removal of arsenic, methylene blue and phosphate by biochar/AlOOH nanocomposite. *Chem. Eng. J.* **2013**, *226*, 286–292. [CrossRef]
23. Ruan, X.C.; Liu, M.Y.; Zeng, Q.F.; Ding, Y.H. Degradation and decolorization of reactive red X-3B aqueous solution by ozone integrated with internal micro-electrolysis. *Sep. Purif. Technol.* **2010**, *74*, 195–201. [CrossRef]
24. Feng, H.; Zhao, D. Preparation and Characterization of a New Class of Starch-Stabilized Bimetallic Nanoparticles for Degradation of Chlorinated Hydrocarbons in Water. *Environ. Sci. Technol.* **2005**, *39*, 3314–3320.

25. Cao, J.; Xu, R.; Tang, H.; Tang, S.; Cao, M. Synthesis of monodispersed CMC-stabilized Fe–Cu bimetal nanoparticles for in situ reductive dechlorination of 1,2,4-trichlorobenzene. *Sci. Total Environ.* **2011**, *409*, 2336–2341. [CrossRef] [PubMed]
26. Wang, J.; Liu, C.; Li, J.; Luo, R.; Hu, X.; Sun, X.; Shen, J.; Han, W.; Wang, L. In situ incorporation of iron-copper bimetallic particles in electrospun carbon nanofibers as an efficient Fenton catalyst. *Appl. Catal. B Environ.* **2017**, *207*, 316–325. [CrossRef]
27. Wan, J.; Li, Z.; Yuan, S.; Lu, X. Removal of Hexachlorobenzene from Kaolin by Electrokinetics Coupled with Cu/Fe PRB. *Pract. Period. Hazard. Toxic Radioact. Waste Manag.* **2010**, *15*, 175–179. [CrossRef]
28. Bransfield, S.J.; Cwiertny, D.M.; Roberts, A.L.; Fairbrother, D.H. Influence of copper loading and surface coverage on the reactivity of granular iron toward 1,1,1-trichloroethane. *Environ. Sci. Technol.* **2006**, *40*, 1485–1490. [CrossRef] [PubMed]
29. Teerakun, M.; Reungsang, A.; Lin, C.; Liao, C. Coupling of zero valent iron and biobarriers for remediation of trichloroethylene in groundwater. *J. Environ. Sci.* **2011**, *23*, 560–567. [CrossRef]
30. Zhou, D.; Li, Y.; Zhang, Y.; Zhang, C.; Li, X.; Chen, Z.; Huang, J.; Li, X.; Flores, G.; Kamon, M. Column test-based optimization of the permeable reactive barrier (PRB) technique for remediating groundwater contaminated by landfill leachates. *J. Contam. Hydrol.* **2014**, *168*, 1–16. [CrossRef] [PubMed]
31. Liang, S.H.; Kao, C.M.; Kuo, Y.C.; Chen, K.F. Application of persulfate-releasing barrier to remediate MTBE and benzene contaminated groundwater. *J. Hazard. Mater.* **2011**, *185*, 1162–1168. [CrossRef] [PubMed]
32. Liang, S.H.; Kao, C.M.; Kuo, Y.C.; Chen, K.F.; Yang, B.M. In situ oxidation of petroleum-hydrocarbon contaminated groundwater using passive ISCO system. *Water Res.* **2011**, *45*, 2496–2506. [CrossRef] [PubMed]
33. Chokejaroenrat, C.; Comfort, S.; Sakulthaew, C.; Dvorak, B. Improving the treatment of non-aqueous phase TCE in low permeability zones with permanganate. *J. Hazard. Mater.* **2014**, *268C*, 177–184. [CrossRef] [PubMed]
34. Garajvrhovac, V.; Kopjar, N.; Raem, D.; Veki, B.; Miljani, S.; Ranogajeckomor, M. Improving the Sweeping Efficiency of Permanganate into Low Permeable Zones To Treat TCE: Experimental Results and Model Development. *Environ. Sci. Technol.* **2013**, *47*, 13031–13038.
35. Jackson, R.E.; Dwarakanath, V.; Meinardus, H.W.; Young, C.M. Mobility control: How injected surfactants and biostimulants may be forced into low-permeability units. *Remediat. J.* **2003**, *13*, 59–66. [CrossRef]
36. Robert, T.; Martel, R.; Conrad, S.H.; Lefebvre, R.; Gabriel, U. Visualization of TCE recovery mechanisms using surfactant-polymer solutions in a two-dimensional heterogeneous sand model. *J. Contam. Hydrol.* **2006**, *86*, 3–31. [CrossRef] [PubMed]
37. Silva, J.A.; Smith, M.M.; Munakata-Marr, J.; Mccray, J.E. The effect of system variables on in situ sweep-efficiency improvements via viscosity modification. *J. Contam. Hydrol.* **2012**, *136–137*, 117–130. [CrossRef] [PubMed]
38. Elder, C.R.; Benson, C.H.; Eykholt, G.R. Effects of heterogeneity on influent and effluent concentrations from horizontal permeable reactive barriers. *Water Resour. Res.* **2002**, *38*, 27:1–27:19. [CrossRef]
39. Zheng, F.; Gao, Y.; Sun, Y.; Shi, X.; Xu, H.; Wu, J. Influence of flow velocity and spatial heterogeneity on DNAPL migration in porous media: Insights from laboratory experiments and numerical modelling. *Hydrogeol. J.* **2015**, *23*, 1703–1718. [CrossRef]
40. Fan, J.H.; Ma, L.M. The pretreatment by the Fe-Cu process for enhancing biological degradability of the mixed wastewater. *J. Hazard. Mater.* **2009**, *164*, 1392–1397. [CrossRef] [PubMed]
41. Wu, S.; Qi, Y.; He, S.; Fan, C.; Dai, B.; Zhou, W.; Lei, G.; Huang, J. Preparation and application of novel catalytic-ceramic-filler in a coupled system for TNT manufacturing wastewater treatment. *Chem. Eng. J.* **2015**, *280*, 417–425. [CrossRef]
42. Wang, K.S.; Lin, C.L.; Wei, M.C.; Liang, H.H.; Li, H.C.; Chang, C.H.; Fang, Y.T.; Chang, S.H. Effects of dissolved oxygen on dye removal by zero-valent iron. *J. Hazard. Mater.* **2010**, *182*, 886–895. [CrossRef] [PubMed]
43. GB/T 14848-93, China. Quality Standard for Groundwater. 1994. Available online: http://kjs.mep.gov.cn/hjbhbz/bzwb/shjbh/shjzlbz/199410/t19941001_66500.shtml (accessed on 22 December 2017).
44. Wu, S.; Qi, Y.; Fan, C.; He, S.; Dai, B.; Huang, J.; Zhou, W.; Gao, L. Application of novel catalytic-ceramic-filler in a coupled system for long-chain dicarboxylic acids manufacturing wastewater treatment. *Chemosphere* **2015**, *144*, 2454–2461. [CrossRef] [PubMed]

45. Jou, C.J.G.; Hsieh, S.C.; Lee, C.L.; Lin, C.; Huang, H.W. Combining zero-valent iron nanoparticles with microwave energy to treat chlorobenzene. *J. Taiwan Inst. Chem. Eng.* **2010**, *41*, 216–220. [CrossRef]
46. Shih, Y.H.; Hsu, C.Y.; Su, Y.F. Reduction of hexachlorobenzene by nanoscale zero-valent iron: Kinetics, pH effect and degradation mechanism. *Sep. Purif. Technol.* **2011**, *76*, 268–274. [CrossRef]
47. Gallard, H.; Laat, J.D. Kinetics of oxidation of chlorobenzenes and phenyl-ureas by Fe(II)/H_2O_2 and Fe(III)/H_2O_2. Evidence of reduction and oxidation reactions of intermediates by Fe(II) or Fe(III). *Chemosphere* **2001**, *42*, 405–413. [CrossRef]
48. Hsiao, Y.L.; Nobe, K. Oxidative reactions of phenol and chlorobenzene with in situ electrogenerated Fentons reagent. *Chem. Eng. Commun.* **1993**, *126*, 97–110. [CrossRef]